

F-16 Ventral Fin Buffet Alleviation Using Piezoelectric Actuators

Joseph S. Browning¹, Richard G. Cobb², Robert A. Canfield³ and Sean K. Miller⁴
Air Force Institute of Technology, Wright-Patterson AFB, Oh, 45433

Buffet-induced vibrations have been problematic for aircraft for many years, and can have a disastrous impact when allowed to continue to the point of structural failure. Early attempts at combating harmful vibrations included relatively passive methods such as structural enhancements and leading edge fences used to minimize the strength of vortices. However, modern techniques have shown greater promise employing active control using piezoelectric actuators. Strategically mounted to the surface of the affected structure, they impart directional strain to reduce the negative effects associated with the strain energy of specific modal vibrations. The Block 15 F-16 ventral fin is representative of an aircraft structure prone to failure when subjected to the buffet field from a Low Altitude Navigation and Targeting Infrared for Night (LANTIRN) pod. However, ventral fin failures pose relatively little risk to the pilot or the aircraft. Therefore, it has great potential as a platform for further investigation into the effectiveness of piezoelectric actuators, which is the subject of this research. Sponsored by the Air Force Research Laboratory (AFRL) in collaboration with the United States Air Force Test Pilot School (TPS), the Air Force Institute of Technology (AFIT) is conducting test flights to demonstrate the effectiveness of active control using piezoelectric actuators for buffet alleviation. This paper documents the hardware design and ground test results in preparation for flight testing, and presents preliminary flight test results.

Nomenclature

AFIT	=	Air Force Institute of Technology
AFRL	=	Air Force Research Laboratory
ASE	=	Aero-Servoelastic Analysis
cRIO	=	National Instruments Inc. CompactRio digital controller hardware
DoD	=	Department of Defense
FEM	=	Finite Element Model
FPGA	=	Field Programmable Gate Array
IGBT	=	Isolated Gate Bi-polar Transistor
LANTIRN	=	Low Altitude Navigation and Targeting Infrared for Night
LQG	=	Linear Quadratic Gaussian
MFC	=	Macro-Fiber Composite
PPF	=	Positive Position Feedback
TPS	=	Test Pilot School (United States Air Force)
g_n	=	filter element gain
n	=	laser vibrometer measurement point
ω_n	=	filter target frequency
w	=	measured deflection for a given mode
ζ	=	filter damping ratio

¹ Captain, USAF, Student, Air Force Institute of Technology, AIAA Member.

² Assistant Professor, Department of Aeronautics and Astronautics, Air Force Institute of Technology, AIAA Associate Fellow.

³ Professor, Department of Aeronautics and Astronautics, Air Force Institute of Technology, AIAA Associate Fellow.

⁴ Laboratory Technician, Department of Aeronautics and Astronautics, Air Force Institute of Technology.

I. Introduction

Active control of structural vibrations, a well explored topic in recent years, has seen application with flexible spacecraft structures¹, helicopter airframes² and even downhill skis with some success. However, the challenge of suppressing structural vibrations in modern high performance aircraft has proven difficult for some time. The capability of modern fighter aircraft to sustain flight at high speeds, high angles of attack, and/or moderate angles of sideslip often results in unsteady, vortical flow around parts of the aircraft's body. In most cases, this flow contains significant levels of energy over a frequency bandwidth common with structural vibration modes of wings, fins, and other surfaces³. The resulting unsteady pressures developed on these surfaces are referred to as buffet. Early fatigue and the generation of cracks result from prolonged exposure to buffeting. In order to sustain operational readiness of affected aircraft, resources must be spent analyzing, repairing, maintaining, and in some cases redesigning structures susceptible to buffet damage.

The most notable cases of buffet-induced vibration problems on aircraft have been with high performance twin-tailed aircraft such as the F-15, F/A-18, and F-22. Buffet loads imposed upon the vertical tails of the F/A-18, for example, led to premature failure of the tail assemblies which not only increased inspection and maintenance costs, but limited the operational capabilities of the aircraft when maneuvering at high angles of attack⁴. A study of F-15 vertical tail failures discovered that fatigue cracking caused by buffet induced vibrations led to undue moisture absorption and corrosion. As with the F/A-18 tails, F-15 buffet problems restricted mission availability and flight maneuvering at high angles of attack. Hanagud perceived an increase in maintenance costs in F-15 operations by as much as \$5-6M per year⁵.



Figure 1. F-16 LANTIRN Pod and Ventral Fin Locations.

Buffet induced vibrations affect more than just vertical tail assemblies. The ventral fin of the F-16 provides an example of an aircraft structure that suffers from this phenomenon. A pair of ventral fins, located on the underside of the fuselage forward of the jet exhaust nozzle as shown in Figure 1, were designed to provide enhanced lateral stability during supersonic flight. During early flights of the first F-16 production models (Block-15 and earlier), the aircraft experienced partial or total ventral fin loss. The main culprit to the failures was turbulence due to abrupt throttle retardations which induce spillage of air from the engine inlet creating oscillatory stress cycles on the ventral fin⁶. Furthermore, these stress cycles were found to be dependent on centerline store configurations. The introduction of the LANTIRN pod, mounted aft of the engine inlet and offset from the aircraft centerline aligned with the ventral fin as shown in Figure 1, saw an increase in fin failures. Figure 2 shows a Block 15 F-16 ventral fin failure following a flight with the LANTIRN pod.



Figure 2. F-16 Block-15 Ventral Fin Failure Example.

Significant research, accomplished by the multinational F/A-18 Buffet Load Alleviation program, has investigated multiple techniques in alleviating buffet loads on the aircraft's vertical tails including the use of piezoelectric actuators. Lazarus, Saarmaa and Agnes⁷ developed an analytical model using distributed, layered piezoelectric actuators bonded to the F/A-18 vertical tail that indicated a 50% reduction in the root-mean-square strain at the root of the tail during simulated flight conditions. Moses investigated active control on a 1/6-scale F/A-18 model in a wind tunnel as part of the Actively Controlled Response of Buffet-Affected Tails (ACROBAT) program and found a reduction of root-mean-square values of tail root strain by as much as 19%⁸.

Despite its promise, the active control of buffet vibrations using piezoelectric actuators has not been tested on actual aircraft beyond the wind tunnel. To date, the only flight-demonstrated effort to employ piezoelectrics for the suppression of vibrations on an aircraft structure was that of the Air Force Research Laboratory in the suppression of acoustic vibrations on a skin panel of the B-1 aircraft⁹. The F-16 Block-15 ventral fin presents an excellent test structure for research of active control in actual flight conditions. Fortunately, ventral fin damage is not critical for safe flight within the nominal F-16 flight envelope (below Mach 1.5). In fact, during past fin damage cases, the pilot had no indication of fin failure during nominal flight conditions. It is important to note that this research is not addressing the failure of the F-16 ventral fin, but takes advantage of susceptibility of Block-15 ventral fins to aerodynamic buffet. Structural modifications solved the buffet problem for Block-30 and later F-16 models.

II. Control Hardware Design

The demonstration of piezoelectric actuators to actively control buffet vibrations on the F-16 ventral fin is based on analytical results developed by Morgenstern¹⁰. Using finite element and aero-servoelastic (ASE) analysis, Morgenstern arrived at design recommendations for piezoelectric actuators based on strain energy density and principle strain vectors for an optimized model. He used the ZAERO ASE software module and flight test data¹⁰ to analyze the first six modes of vibration and highlighted the first, second, and fourth modes as the most critical to ventral fin failure. The work documented herein is the physical implementation of Morgenstern's initial design and the corresponding flight test results.

Morgenstern's investigation into the effectiveness of piezoelectric actuators for the F-16 ventral fin began with an accurate finite element model (FEM). The model was tuned and optimized to match published modal parameters for the fin and was then analyzed to determine strain energy profiles for the first five modes of vibration. The three most critical modes were determined through an evaluation of historical flight test data detailing the relative dominance of each mode and the ventral fin failure history, as well as an evaluation of the aeroelastic characteristics of the fin's FEM. Piezoelectric actuators were designed and integrated into the FEM for areas of maximum strain using a piezo-thermal analogy within MSC.Nastran. Figure 3 illustrates these areas for the first and second vibration modes. Morgenstern's research showed that piezoelectric actuators specifically located in areas of elevated strain with the principal piezo effect direction aligned with the principal strain vectors provided for the highest probability of success.

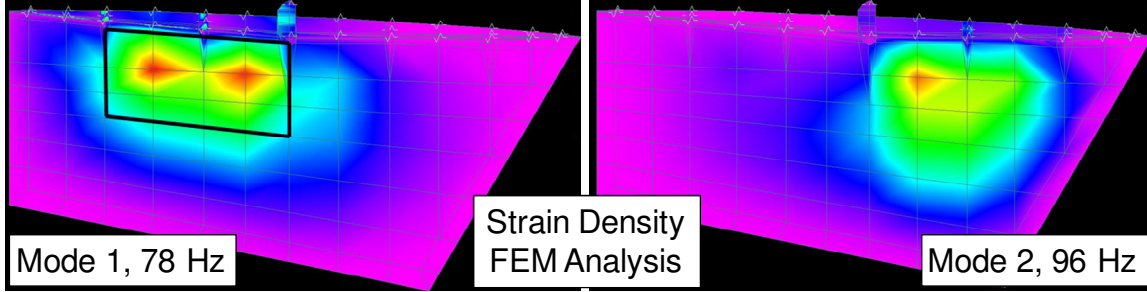


Figure 3. Finite Element Analysis Showing Areas on the Ventral Fin of Elevated Strain Density.

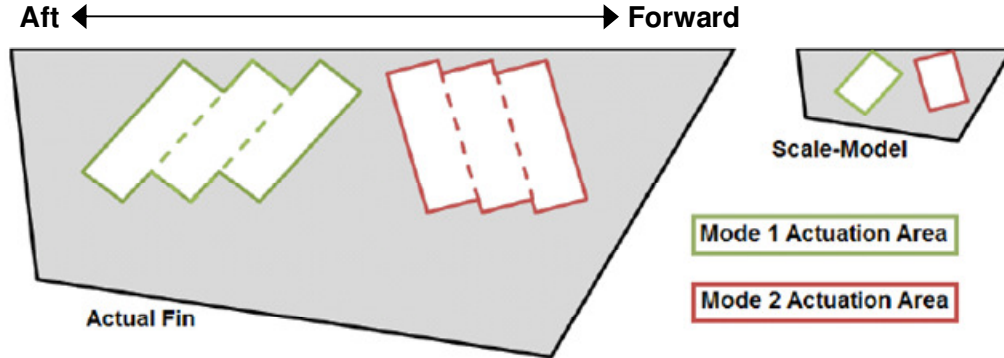


Figure 4. Piezoelectric Actuator Locations for the Ventral Fin.

This research carries the recommendations of Morgenstern through the design of piezoelectric actuators and sensors and a closed-loop control system. Modes 1 and 2, the first symmetric and antisymmetric modes of vibration respectively, were chosen as targets for this research based on Morgenstern's recommendations and on performance predictions of a single layer of piezoelectric actuators. Because the strain energy of each mode was distributed in separate areas, actuators could be distributed in two arrays designed specifically to target the respective mode. Orthotropic (d_{33} charge constant) Macro-Fiber Composite (MFC) piezoelectric actuators manufactured by Smart-Materials Inc. were chosen as the actuators. Collocated piezoelectric sensors embedded in the actuators near the center of each actuation area were designed to provide feedback for closed-loop control. The actuator/sensor pairs were aligned according principal strain directions of the mode of interest as shown in Figure 4.

An aluminum scaled model of the ventral fin, as shown in Figures 4 and 6, was also used to prototype feedback control hardware and software, before the piezoelectric hardware was installed on the actual ventral fin. Additionally, as a verification step prior to piezoelectric hardware installation on the flight fin, the principal strain directions were experimentally determined using a central difference method by measuring the curvature (2^{nd} derivative of displacement) across the actuator areas shown in Figure 4. The strain was computed using Eq 1, where w represents the measured deflection for a given mode and n represents the measurement point. Deflections were measured using a scanning laser vibrometer with the fin excited using a electrodynamic shaker attached to the free edge of the fin via a lightweight stinger driven by a pseudo-random white noise signal. At each measurement point:

$$\left(\frac{d^2w}{dx^2}\right)_n = \frac{\left(\frac{dw}{dx}\right)_{n-1} - \left(\frac{dw}{dx}\right)_{n+1}}{x_{n+1} - x_{n-1}} = \text{Strain}_n \quad (1)$$

where the slope at each measurement point n was calculated from

$$\left(\frac{dw}{dx}\right)_n = \frac{w_{n+1} - w_{n-1}}{x_{n+1} - x_{n-1}}$$

The experimentally determined principal strain vectors correlated well with the FEM predictions, as shown in Figure 5, and enabled the accurate alignment of the piezoelectric actuation fibers in the direction of principal strain within each targeted area. The actuators and collocated sensors were then installed on the flight Block-15 ventral fin, as shown in Figure 6, using a surface vacuum bagging technique and high performance epoxy.

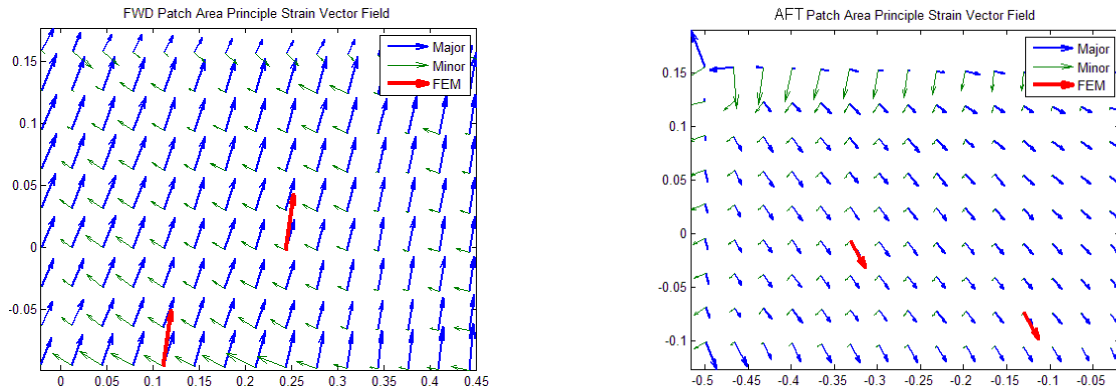


Figure 5. Experimental to FEM Comparison of Vector Strain Field at Piezo Actuator Locations.

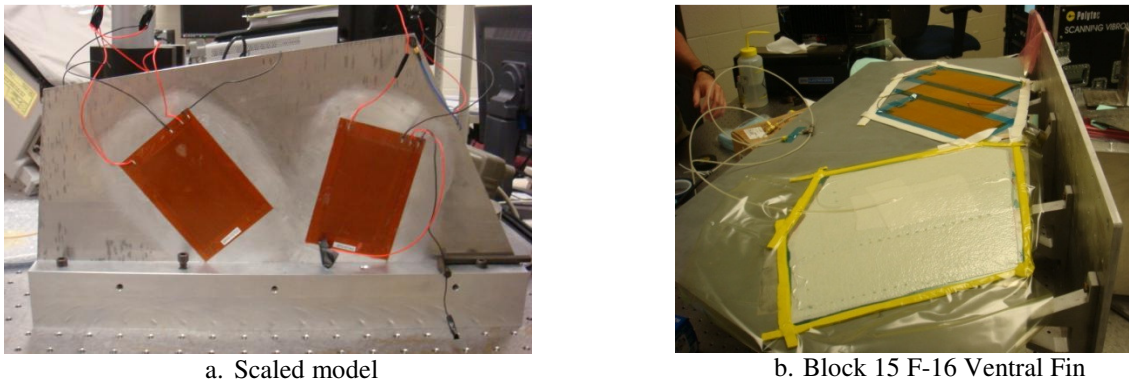


Figure 6. Piezoelectric Actuator/Sensor Installation.

Drive Amplifier Design

Because the impedance of piezoelectric actuators is primarily reactive, their load on a circuit regenerates a significant amount of power to the driving amplifier. The reactive impedance also implies that the driving amplifier must be able to handle significantly higher voltages and circulating currents than suggested by the real power requirements of the actuators. Because of this, a switching amplifier topology was chosen as the drive amplifier. The switching amplifier recovers a substantial amount of stored energy during the discharge of a capacitive load as recycled power, which when routed to series-connected capacitors can be reused during subsequent load discharges without causing circuit noise. However, a suitable off-the-shelf drive amplifier was not available; thus, a custom amplifier was designed and built for this research.

The MFC piezoelectric actuators used in this research were capable of +1500 to -500 volts. To simplify the control algorithm and drive amplifier design, the actuators were limited to ± 500 volts. Because the system was flight tested on an F-16D aircraft, the amplifier was made compatible with 28 volt DC (18V - 32V range) aircraft power and able to operate under elevated load factor (G) up to 30,000 feet pressure altitude. Closed loop control signals from a digital controller, described in the next section, were designed at ± 5 volt AC. Bit selectable system operation commands, an adjustable attenuation circuit, and signal conditioning for the piezoelectric sensor signals on the ventral fin were also housed within the amplifier electronics.

The primary consideration for the amplifier design was power efficiency. A ‘Class D’ type topology was chosen for its characteristically low heat dissipation stemming from the use of fully ‘on’ or fully ‘off’ output transistors. The output stage of a Class-D amplifier can be a half-bridge or full-bridge design which typically employs a Metal-Oxide-Semiconductor Field Effect Transistor (MOSFET) or an Isolated Gate Bi-polar Transistor (IGBT). The more stable full-bridge design using IGBT’s and off-the-shelf Semikron driver circuits were used in the design. The driver circuits required pulse width modulated (PWM) drive signals; therefore, additional circuitry was developed to convert the analog control signal from the digital controller to a suitable PWM signal. The PWM generation was accomplished by comparing a 20 kHz triangle waveform to the analog input signal. An EMI filter was added to the power input stage to offset EMF/EMI problems with the 20 kHz switching frequency.

The piezoelectric actuators possessed a nominal capacitance of 0.216uF (at 100 Hz) as seen by the amplifier output stage. Each actuator array, forward and aft, were comprised of six total actuators wired in parallel resulting in an estimated 1.3 uF capacitance. DC bus “fill” capacitors rated at ten times the piezoelectric load were used to complete the circuit. The amplifier was rated at twice the DC bus voltage to enhance system robustness. The completed schematic for the amplifier is shown in Figure 7. A representative transfer function for one channel of the amplifier, as shown in Figure 8, illustrates the 400 Hz bandwidth of each amplifier.

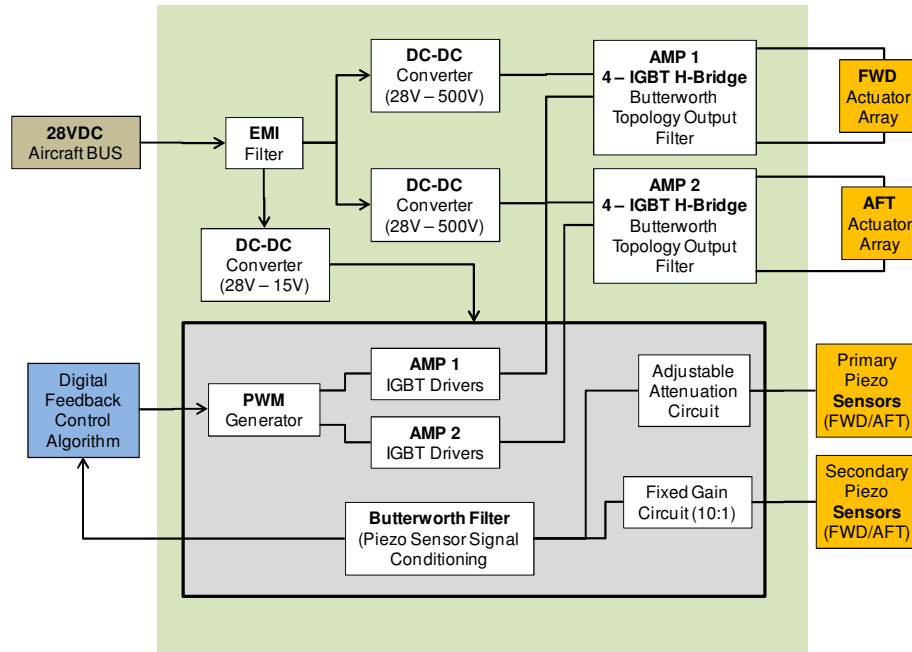


Figure 7. AFIT Custom Built Power Amplifier Schematic.

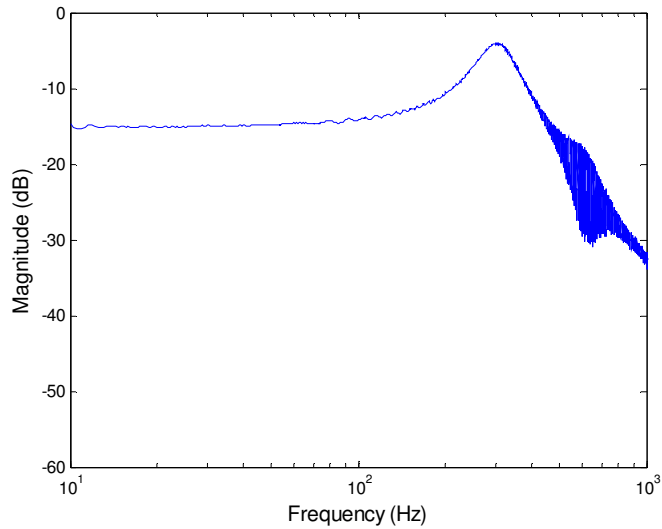


Figure 8. Piezoelectric Drive Electronics Frequency Response.

Controller Design

The National Instruments Inc. Compact RIO (cRIO) digital controller using a LabView software package was chosen to implement digital feedback control algorithms and to serve as an interface to the piezoelectric drive electronics. The digital controller A/D input module received piezoelectric sensor signals from the amplifier after signal conditioning. The controller sampled at 10 kHz. The D/A output module routed the feedback signal to the amplifier to drive the actuators. A dSPACE digital controller combined with MATLAB’s Simulink was also used in the laboratory to benchmark performance. The entire system is illustrated in the block diagram of Figure 9.

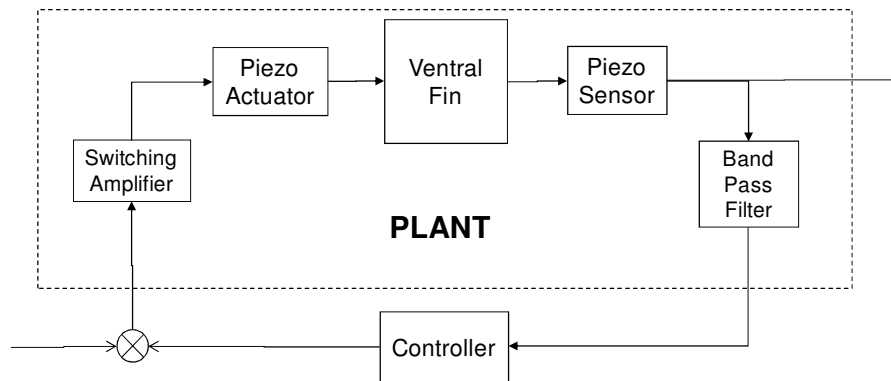


Figure 9. Plant Model

Feedback control techniques used in this research included two types of digital techniques, both using collocated piezoelectric sensors for feedback control. Previous buffet alleviation research^{3,4,5,7,8} incorporated acceleration feedback control using accelerometers as the primary sensor. This research focused on piezoelectric sensors for feedback control because the sensors could be collocated with the piezoelectric actuators simplifying control design. Actuators and sensors of previous buffet alleviation research were not collocated in part because areas of maximum strain energy for a particular mode did not necessarily coincide with the optimum location of an acceleration feedback sensor. Several advantages exist, however, with collocated designs including favorable closed-loop stability margins. Collocated sensors and actuators lead to symmetric transfer functions where poles and zeros appear in pairs for each natural frequency of the system. Preumont determined that this property guarantees the asymptotic stability of a wide class of single-input single-output (SISO) systems because the root loci remain entirely in the left-half plane¹².

The first digital control technique involved positive position feedback (PPF), as presented by Goh and Caughy¹, for the modes of interest. Each actuator array used an independent PPF algorithm comprised of n parallel second order filter elements following Eq 2 below. The gain of each second order filter element (g_n) was set to provide a minimum 6 dB gain margin and 45 degree phase margin. The stability margins were based on the open-loop data and the analytically predicted filter response. The frequency (ω_n) was set to approximately match the modes of interest, and the damping value for the filter (ζ) was set to 0.5 for each filter element.

$$G_{PPF}(s) = \sum_n \frac{-g_n \omega_n^2}{s^2 + 2\zeta \omega_n s + \omega_n^2} \quad (2)$$

The forward array PPF algorithm consisted of three of these filters oriented in parallel each targeting the first mode (78 Hz), second mode (96 Hz), and the third mode (169 Hz), respectively. The aft array PPF algorithm used only a single filter targeting the second mode. These were chosen after laboratory testing revealed an optimum configuration of PPF filters for each array. The PPF filters were easily implemented in the cRIO digital controller as finite difference equations placed on the Field Programmable Gate Array (FPGA) housed in the cRIO. Directly programming the FPGA enabled faster sample rates and fixed-step computation times ensuring deterministic control of the plant. A bode plot of each compensator is shown in Figure 10. The PPF algorithms were non adaptive; once compiled to the digital controller, the target frequency of each filter could not be changed in real-time.

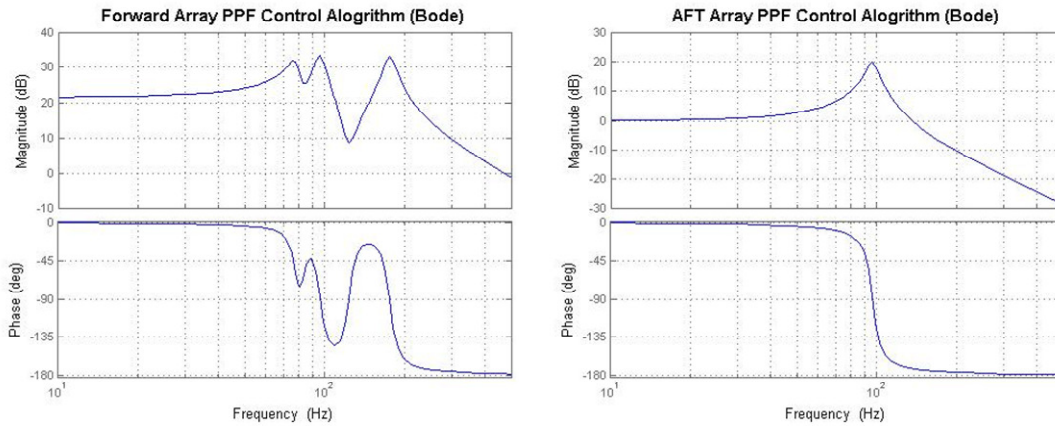


Figure 10. Positive Position Feedback Algorithms (Bode Diagrams)

The second digital control technique incorporated an 8th order Linear Quadratic Gaussian (LQG) design. LQG, a form of the modern H_2 control method, are commonly considered in vibration control problems mostly due to stability guarantees associated with robust methods. The LQG regulator has been popular in vibration control problems in that it balances performance and control effort while accounting for process and measurement noise. An 8th order LQG compensator was selected for this research based on the available bandwidth of the amplifier and its ability to effectively control lower frequency vibration modes of the ventral fin. Each actuator/sensor array used an independent LQG algorithm for control. The LQG compensator was based on an experimentally derived open-loop model. The Eigenstructure Realization Algorithm, implemented in MATLAB, was used to extract a state-space model from the measured open-loop frequency responses. The LQG compensator was weighted evenly and then reduced so as to only target the first three modes (78, 96, and 169 Hz). Figure 11 shows the bode representation of each LQG compensator.

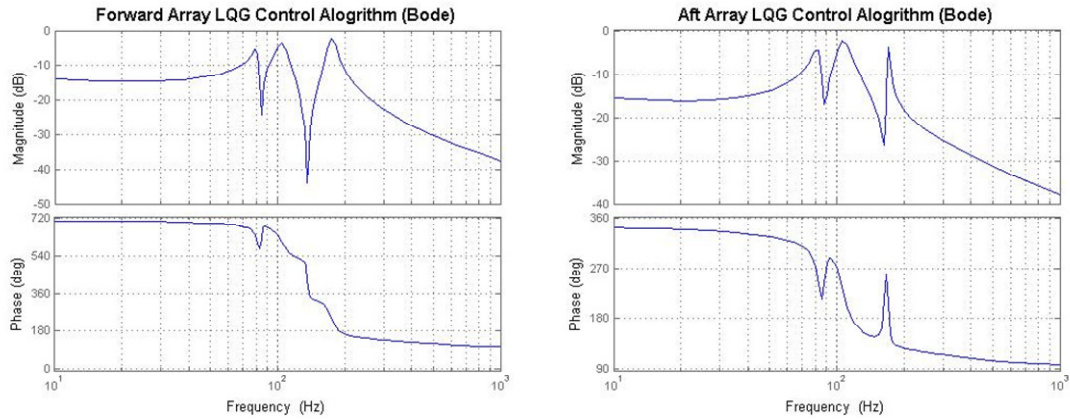


Figure 11. Linear Quadratic Gaussian Algorithms (Bode Diagrams)

Unfortunately, the LQG methods could only be used with the laboratory dSPACE digital controller because the 8th order transfer function could not be successfully implemented on the FPGA or cRIO efficiently. Results of LQG control reference laboratory testing only.

III. Ground Test Results

Laboratory Results

Before installing on the airframe, open and closed-loop frequency response plots were recorded. Data was collected using both a scanning laser vibrometer (ground tests only) and voltages from the collocated piezoelectric sensors. Figure 12 shows the laboratory setup where the fin is mounted on an optical bench. The open-loop transfer function of the forward actuator/sensor array is shown in Figure 13. The collocated attributes of the actuator/sensor pair can be seen in the grouping of pole-zero pairs of the frequency response. A special mount, designed to imitate the aircraft fuselage interface as closely as possible, was made to secure the ventral fin to the optics table and provide a stable platform for testing. As previously discussed, several control schemes were tested. For brevity, only two will be discussed. The first was developed using a pure analog feedback circuit and high power lab amplifiers (not suitable for flight). This test provided a baseline with which to compare the flight electronics. Figure 13 shows the sample results using the forward array and sensor, and high gain analog feedback. A greater than 20dB reduction was achieved for mode 2, with smaller reductions to the other modes. It was anticipated that similar performance could be achieved with the flight piezo amplifier and digital controller. A second test was done applying an 8th order LQG based digital controller to the both the forward and aft actuator arrays as shown in Figure 14. For this test, the digital control signal was implemented on a non-flight dSPACE digital controller, since the LQG algorithm could not be implemented on the flight cRIO controller. Again, significant (>20dB) attenuation was achieved for the first few modes. A third test was accomplished using the flight cRIO hardware and the PPF algorithms for the forward and aft actuator arrays as shown in Figure 15. Attenuation (>15dB) of the targeted modes was achieved in each case. Having successfully demonstrated closed-loop control in the lab with flight hardware and control algorithms, the next step was to mount the hardware on the airframe and continue testing.

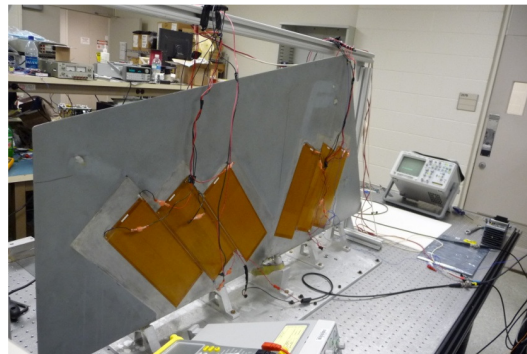


Figure 12. Laboratory Setup Showing Instrumented Block-15 F-16 Ventral Fin

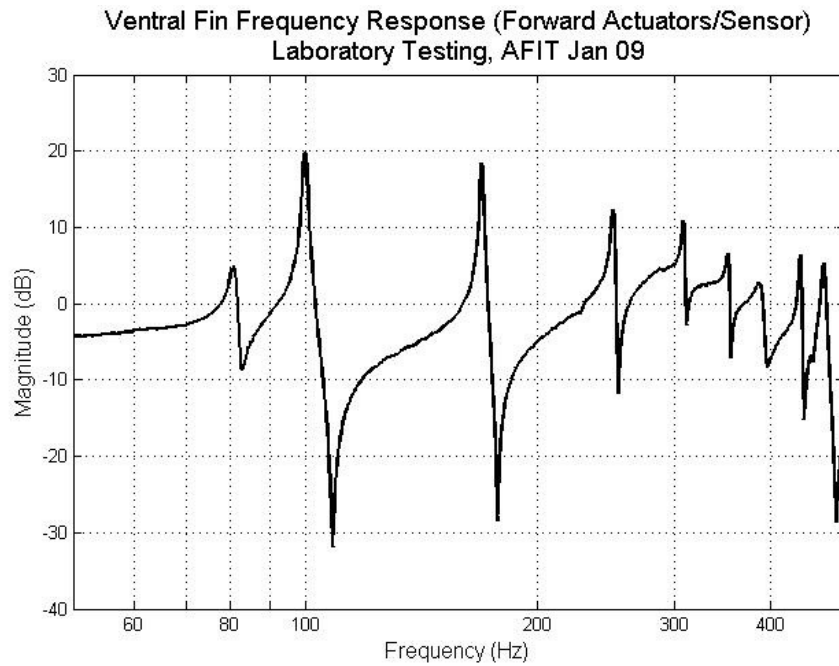


Figure 13. Ventral Fin Frequency Response during Laboratory Testing
Input Excitation: Frequency Chirp to Forward Actuators
Output Measurement from Forward Array Sensor

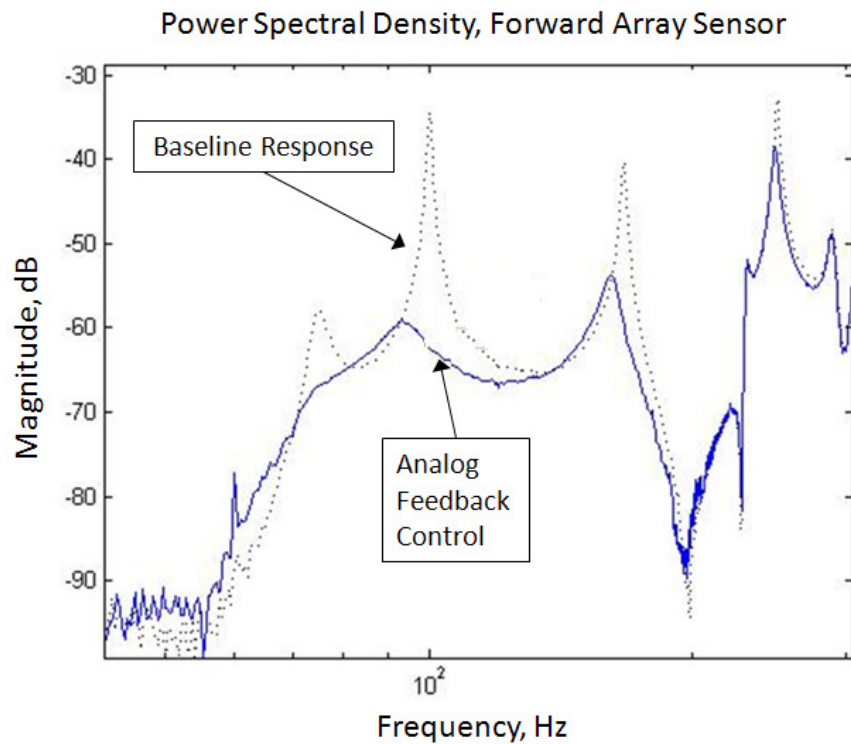


Figure 14. Comparison of Open and Closed-Loop Results

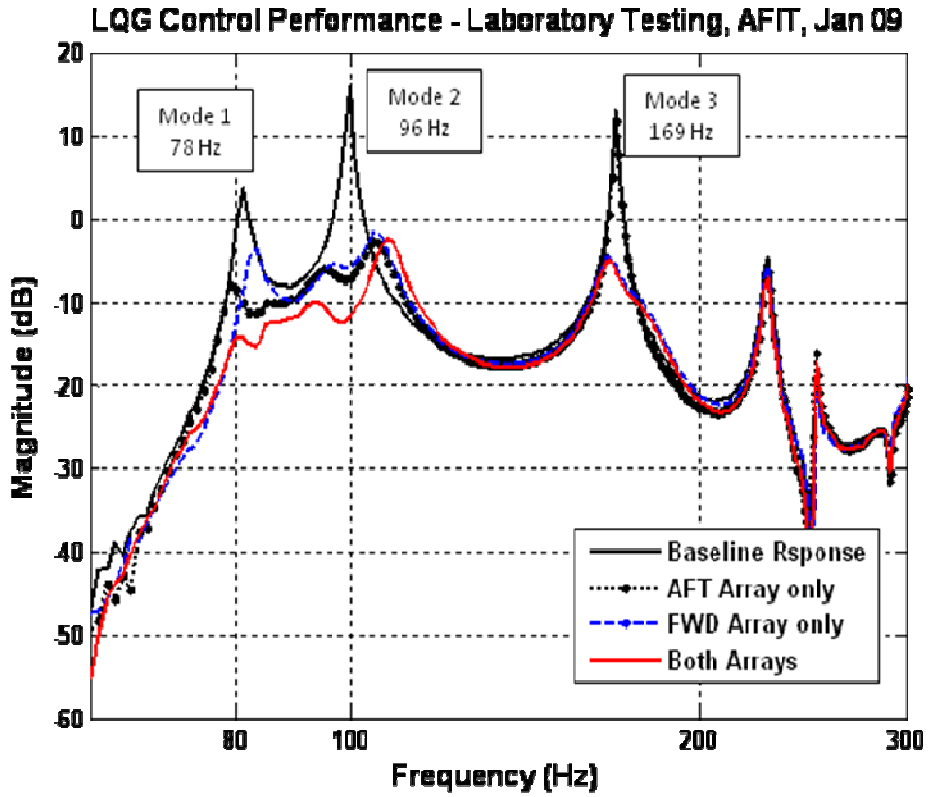


Figure 15. Lab Test Results, 8th Order LQG Digital Control

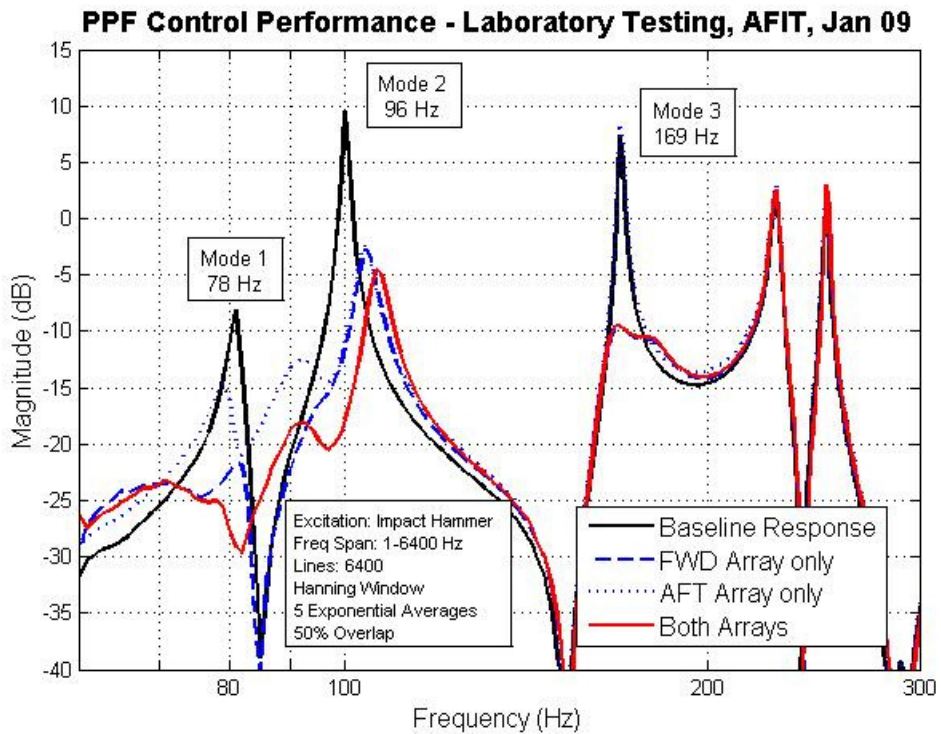


Figure 16. Lab Test Results, PPF Digital Control

Ground System Checkout Results

The instrumented ventral fin, amplifier assembly, and digital controller were installed on a Block-30 F-16D aircraft at Edwards AFB, CA, as part of the ACTIVE FIN test project at TPS. Once installed on the airframe, open and closed-loop frequency response plots were recorded. Figure 17 shows the test aircraft with the instrumented Block-15 ventral fin installed along with the drive amplifier and digital controller in the ammo bay (used as an avionics compartment) behind the rear cockpit. A handheld PC was mounted in the rear cockpit and interfaced with the cRIO controller to provide the aircrew with system operation control during testing. Data was collected using only the voltages recorded from the collocated piezoelectric sensors. The open-loop transfer function of the forward actuator/sensor array is shown in Figure 18. For comparison purposes, the non-collocated sensor response at the aft array is also included in this figure. Figures 19 and 20 show the achieved performance of the forward and aft actuator arrays, respectively. For this test, the cRIO digital controller used only the 2nd order PPF control laws developed during laboratory testing. In each case, >10dB reduction was achieved in the 96Hz mode.



Figure 17. ACTIVE FIN Installed on Test Aircraft. (photos courtesy of Edwards AFB, PA)

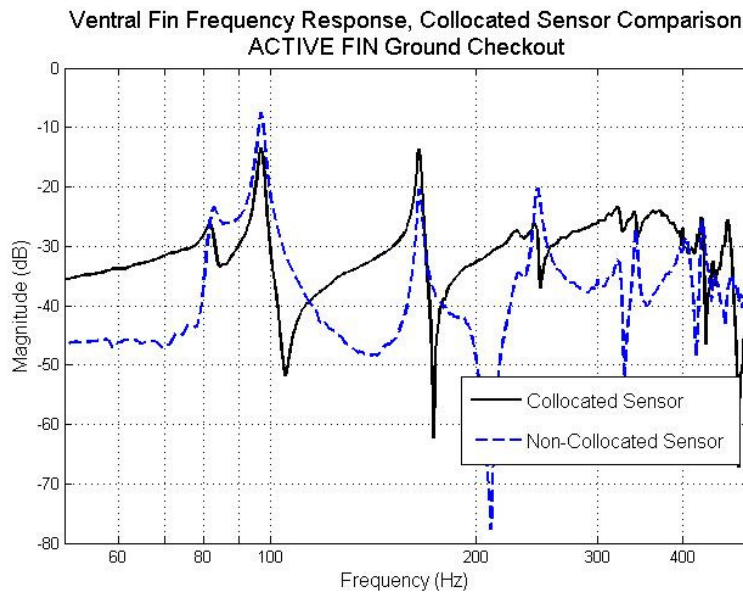


Figure 18. Ventral Fin Frequency Response after Aircraft Installation
Input Excitation: Frequency Chirp to Forward Actuators
Output Measurement from Forward and Aft Array Sensors

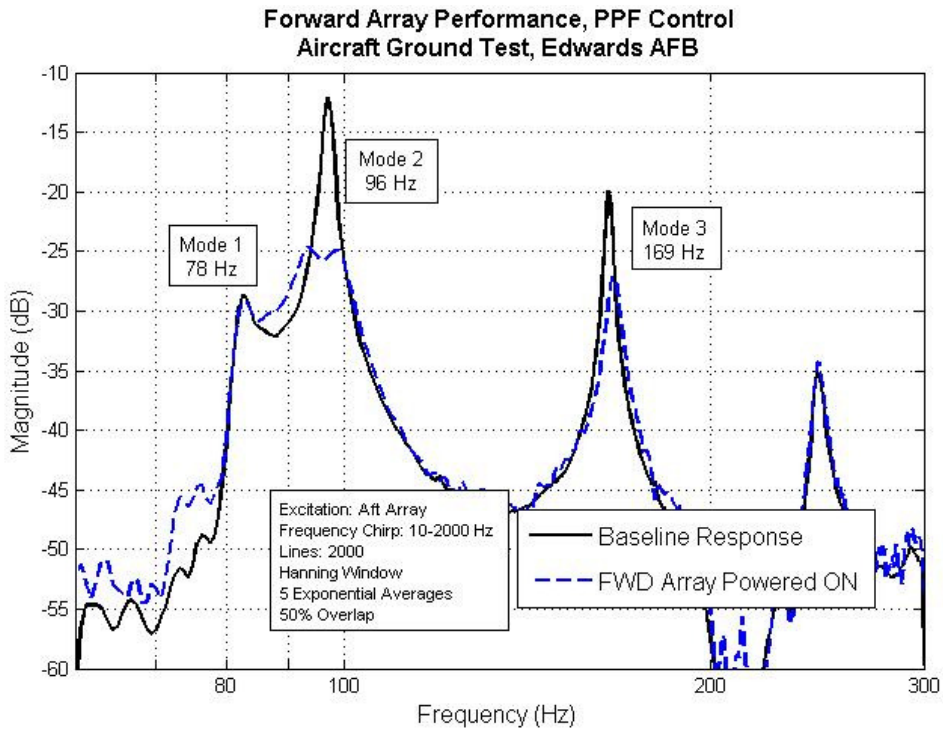


Figure 19. ACTIVE FIN Ground System Checkout, Forward Array Performance

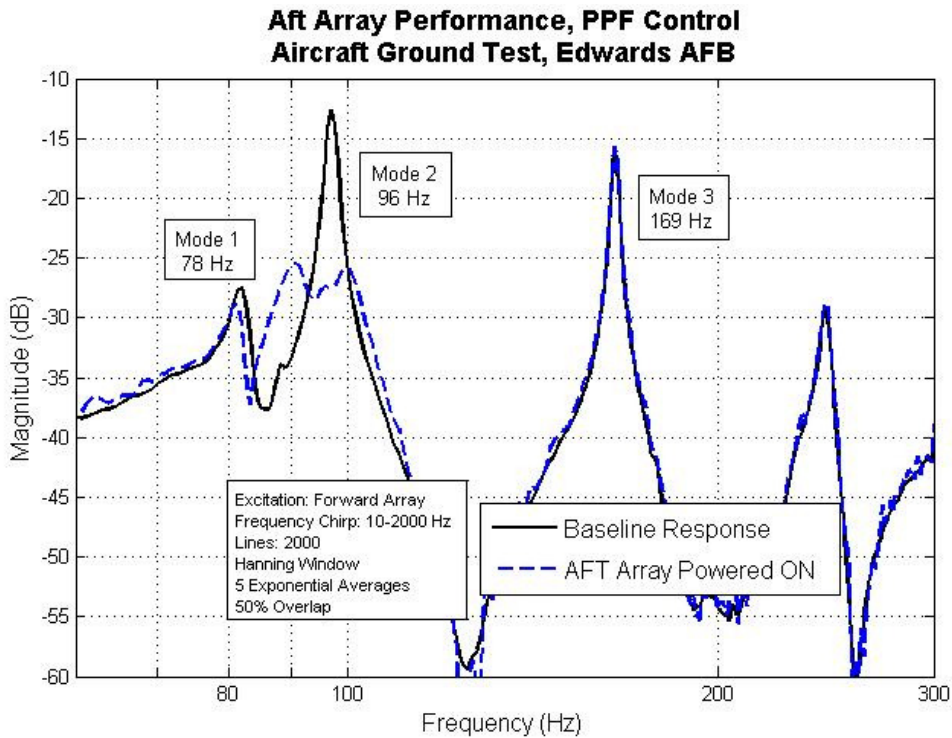


Figure 20. ACTIVE FIN Ground System Checkout, Aft Array Performance

IV. Flight Test Activities

The flight test, conducted under the ACTIVE FIN project by TPS, consisted of two basic phases: open-loop flight characterization, and closed-loop digital control assessment. The test aircraft was configured with the test Block-15 ventral fin, two external wing fuel tanks, and a LANTIRN pod on station 5R as shown in Figure 21. All flight tests were flown during conditions known to produce measurable buffet in the ventral fin. These conditions, determined during the HAVE PUFF test project¹¹ at TPS during 2005, included points at high dynamic pressure: at or below 15,000 feet pressure altitude and between 0.70 and 0.95 Mach. The ACTIVE FIN envelope explored test points up to Mach 1.05 to fully characterize the transonic region. Maneuvering consisted primarily of level trim shots (straight and level, constant speed) and level, constant-load factor turns to a maximum of 5-G. Varying load factor test conditions were used to vary aircraft angle of attack at constant Mach and altitude. Figure 21 provides estimated test conditions for each test phase. Data during the flight tests, including piezoelectric sensor signals and aircraft state parameters, were recorded using an onboard Data Acquisition System (DAS) at a rate of 6.5 kHz. The flight test phase was conducted in April 2009, so only a portion of the flight results were available for inclusion in this paper.



Figure 21. ACTIVE FIN Instrumented Test Aircraft. (photos courtesy of Edwards AFB, PA)

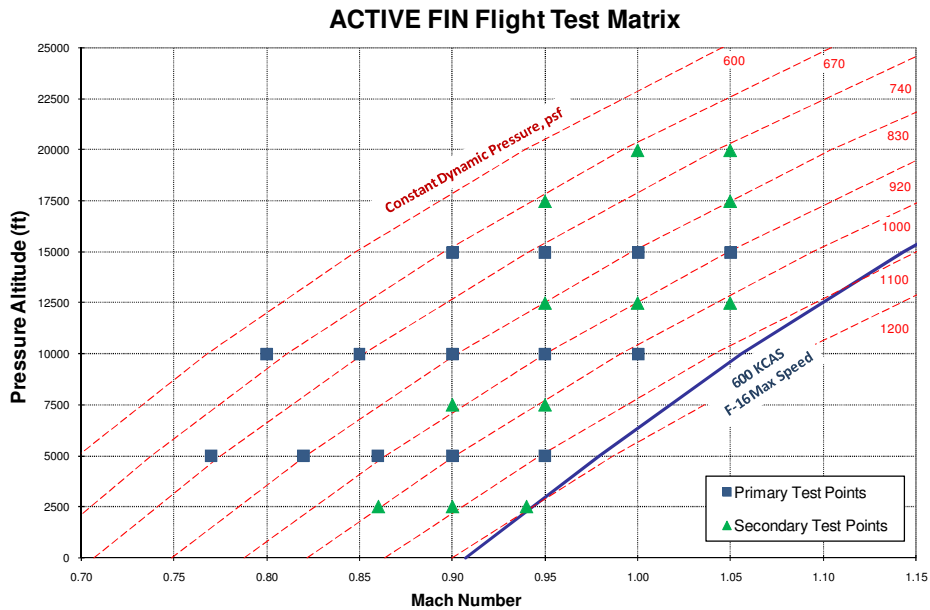


Figure 22. Planned Flight Test Conditions.

The flight characterization phase was intended to characterize the frequency response of the ventral fin within the range of intended test conditions (altitude, Mach, G-level). During this phase, the piezoelectric actuators were not used to control vibration. Piezoelectric sensor signal levels were monitored and recorded to assess vibration levels. Post-test data reduction of the sensor signals was used to determine natural frequencies, the power spectrum, and to narrow down specific flight conditions that produce measurable fin buffet. The natural frequencies shifted compared to laboratory test data, as listed in Table 1, due to aerodynamic influence and changes in boundary conditions (how the fin is mounted to the aircraft). This shift dictated the settings when programming the non-adaptive digital control algorithms. The power spectrum served as the truth for the next phases of test. Appropriate safety limits (saturation limits) were coded into the control algorithms based on sensor signal power spectrum magnitudes experienced during the characterization phase to ensure divergent conditions are avoided. Depending on aircraft availability and other scheduling conflicts, the ‘powered actuator’ test envelope may be focused to conditions determined to provide the highest levels of buffet in the ventral fin.

Table 1. Ventral Fin Natural Frequency Comparison*

	Mode 1	Mode 2	Mode 3	Mode 4
Laboratory Testing	85	100	165	251
Flight Testing	78	96	169	251

* data given in hertz

To date, only a limited amount of data was collected on the open and closed-loop responses in flight. Early indications showed that ~5 dB of attenuation was achieved, significantly less than the results achieved during ground tests. Because the flight tests are still ongoing, the full results of these tests, and the lessons learned will be reported in a subsequent report.

V. Conclusions

The development of an autonomous active control system using collocated piezoelectric actuators and sensors to alleviate the buffet response of the vibration modes of the Block-15 F-16 ventral fin during ground and flight tests were presented. Seven distinct tasks were completed as part of this research. First, piezoelectric actuators were applied in the specification of appropriate sensors and actuators for the ventral fin. Several deviations were necessary, including individual actuator size and orientation and selection of piezoelectric feedback sensors versus acceleration feedback, to tailor the piezoelectric elements for practical application on the ventral fin. Second, a switching amplifier capable of supporting the unique reactive load of piezoelectric actuators was designed and built. Next, using a scale-model of the fin, control algorithms were developed according to several methodologies mentioned above in order to deliver a desired vibration response at the location of a given actuator. Using a scale-model aided in better understanding the problem and in avoiding issues with installation of piezoelectric hardware onto the actual test article. A mount for the ventral fin was designed and built in order to accomplish ground vibrations tests using a scanning laser vibrometer and electromagnetic shaker. Before being instrumented with piezoelectric hardware, the ventral fin was analyzed to verify principal strain directions calculated by Morgenstern. National Instruments Inc. hardware was programmed using the LabView software package to implement control algorithms and cockpit user interfaces during ground and flight test activities. The entire control system, including controller hardware, switching amplifier, and ventral fin instrumented with all piezoelectric hardware was ground tested to verify total control system performance and stability. Finally, the control system was installed on a Block-30 F-16D, tested, and critiqued by the United States Air Force Test Pilot School.

Acknowledgments

Special thanks to the AFIT model shop for the fabrication of the amplifier electronics flight assembly and to the ACTIVE FIN flight test team at the USAF Test Pilot School.

References

¹Goh, C. J. and T. K. Caughey. “On the Stability Problem Caused by Finite Actuator Dynamics in the Collocated Control of Large Space Structures”. *International Journal of Control*, Vol. 41(No. 3):787-802, 1985.

²Connolly, A. J., M. Green, J. F. Chicharo, and R. R. Bitmead. "The Design of LQG & H(infinity) Controllers for use in Active Vibration Control & Narrow Band Disturbance Rejection". *Proc. of the 34th Conference on Decision and Control, New Orleans, LA*, 2982{2987, December 1995.

³Burnham, J. K., D. M. Pitt., E. V. White, D. A. Henderson, and R. W. Moses. "An Advanced Buffet Load Alleviation System". *42nd AIAA/ASME/ASCE/AHS/ASC Structures, Structural Dynamics, and Materials Conference and Exhibit*, Seattle, WA, (AIAA-2001-1666), April 16-19 2001.

⁴Sheta, Essam F. et al. *An Active Smart Material Control System for F/A-18 Buffet Alleviation*. Technical report, International Forum on Aeroelasticity and Structural Dynamics, Amsterdam, Netherlands, June 2003.

⁵Hanagud, Sathyanaraya. *F-15 Tail Buffet Alleviation: A Smart Structures Approach*. Technical report, School of Aerospace Engineering, Georgia Institute of Technology, Atlanta, GA 30332, December 1998.

⁶van Tongeren, J.H., C.J. Lof, J.J. Meijer, and E.G.M. Geurts. *F-16 Ventral Fins Analysis*. Technical Report NLR-CR-99366, National Aerospace Laboratory, Amsterdam, The Netherlands, August 1999.

⁷Lazarus, K. B., E. Saarmaa, and G. S. Agnes. "An Active Smart Material System for Buffet Load Alleviation". *SPIE's 2nd Annual International Symposium on Smart Structures and Materials*, Vol. 2447:179-192, 1995.

⁸Moses, Robert W. *NASA Langley Research Center's Contributions to International Active Buffet Alleviation Programs*. Technical report, Aeroelasticity Branch, NASA Langley Research Center, Hampton, VA, 1999.

⁹Falangas, Eric T. et al. *Piezoceramic Actuator Active Vibration Suppression System B-1B Flight Demonstration Program*. Technical Report AFRL-VA-WP-TR-1999-3011, Air Vehicles Directorate, Air Force Research Laboratory, AFMC, Wright-Patterson AFB, Ohio, January 1998.

¹⁰Morgenstern, Shawn D., *Alleviation of Buffet-Induced Vibration using Piezoelectric Actuators*. Masters thesis, Graduate School of Engineering, Air Force Institute of Technology, Wright-Patterson AFB, OH, February 2006, AFIT/GAE/ENY/06-M25.

¹¹Morgenstern, Shawn D., Aaron A. Tucker, Heather C. Giebner, Aniello Violetti, and Dick Wong. *Limited Characterization of Dual Bimorph Synthetic Jet Actuators: Aeroelastic Load Control - Phase I, Project HAVE PUFF*. Technical Information Memorandum AFFTC-TIM-05-07, Air Force Flight Test Center, Edwards AFB, CA 93524, December 2005.

¹²Preumont, Andre. *Vibration Control of Active Structures*. Kluwer Academic Publishers, 2nd edition, 2002.